Th N104 09

# Global Anisotropic FWI

H.A. Debens* (Imperial College London), M.R. Warner (Imperial College London) & A. Umpleby (Imperial College London)

## SUMMARY

Seismic anisotropy influences both the kinematics and dynamics of seismic waveforms. As such, if not taken into account properly during multi-parameter full-waveform seismic inversion (FWI), the anisotropy can manifest itself as significant error in the recovered P-wave velocity model. With this in mind we demonstrate a hybrid local-global inversion scheme to extract the low-wavenumber component of the anisotropy in combination with a high-resolution P-wave velocity model. This can then be followed by conventional local inversion for one or both parameters. Our results demonstrate that this technique suppresses the cross-talk between anisotropy and velocity, whilst producing more accurate final models for both parameters.

## Introduction

In a commercial context, full-waveform seismic inversion (FWI) has been used principally to recover P-wave seismic velocity, although any parameter that has an influence upon the observed seismic wavefield can in principle be estimated by FWI. For most 3D field datasets, it is necessary to include the kinematic effects of P-wave anisotropy in order to get the full benefit of FWI and to depth migrate the reflection data accurately. This anisotropy model is typically generated using reflection travel-time tomography, but it is of course possible to invert for both P-wave velocity and anisotropy during FWI, and this approach is becoming more common (da Silva et al., 2014).

Conventional FWI proceeds using a purely local inversion scheme, and this can be problematic if the starting velocity and anisotropy models are not already accurate. In this paper, we explore an alternative strategy in which we combine local and global inversion methods to recover a global long-wavelength model of anisotropy together with a local high-resolution model of velocity. Hybrid inversion is feasible (Ji and Singh, 2005), even for large 3D datasets, because the required anisotropy model is much smoother than the velocity model, and so can be represented by rather few independent parameters.

## Method

Figure 1a illustrates schematically some of the difficulties of using local inversion to recover anisotropy. In general, there is a strong trade-off between velocity and anisotropy such that the data-misfit surface tends to form narrow troughs that are oblique to both velocity and anisotropy axes. Points A, B & C in Figure 1a represent three possible starting models; the contours show the misfit surface. For model A, the best strategy is to invert for velocity while holding the anisotropy constant; for model B, it is best to invert for anisotropy while holding velocity constant; and for model C, it is best to invert for both parameters simultaneously. Applying the wrong strategy will often lead to a worse fit to the true model.

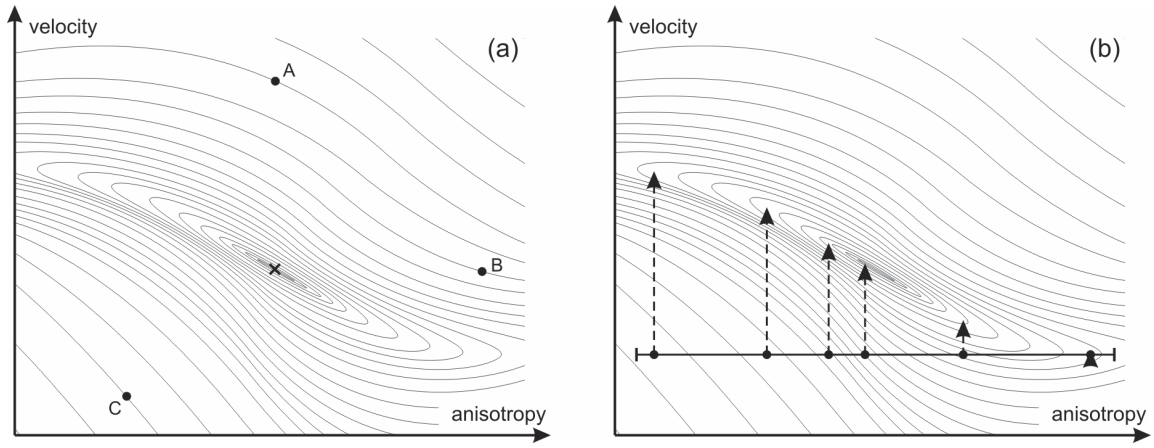


***Figure 1*** *(a) Local inversion for three start models; (b) Global inversion for one velocity model.*

Figure 1b shows an alternative approach. Here the inversion begins from just one velocity model represented by the horizontal line. Several anisotropy models are then chosen, within some bounds, as represented by the points. Local inversion for velocity is then applied to each model as represented by the arrows. The final misfit of each inverted model is then examined, and a new velocity model, and multiple new anisotropy models, are chosen statistically on the basis of these fits. In Figure 1b, these new models will tend to be chosen close to the end points of the central two models since these now have the smallest misfit. We have used quantum particle swarm optimisation (QPSO) (Sun et al., 2004) to update the models. For a practical scheme, we found that it is only necessary to use three local iterations per global iteration, to use about twenty global iterations in total, and to use a population that is of a similar size to the number of anisotropy parameters required. Even in large 3D models, the latter is seldom more a few tens of parameters for the long-wavelength anisotropy model.

**Example**

The model we chose to demonstrate the hybrid local-global approach is the upper portion of the synthetic 2D Marmousi model (Bourgeois et al., 1990), selected for its complex velocity structure (Figure 2j). The anisotropic parameterisation we chose to invert for is vertical transverse isotropy (VTI), partly because of its common occurrence worldwide but also for its relative simplicity. We designed a complimentary smoothly-varying anisotropy model for Thomsen's (1986) epsilon parameter (Figure 2e) that cross-cuts the strata of the velocity model and is decoupled from the velocity values. Because the velocity and epsilon models have different structure here, this model allows for the reliable assessment of cross-talk and coupling between the two parameters. In this example, Thomsen's (1986) delta parameter is left unchanged at a zero value.

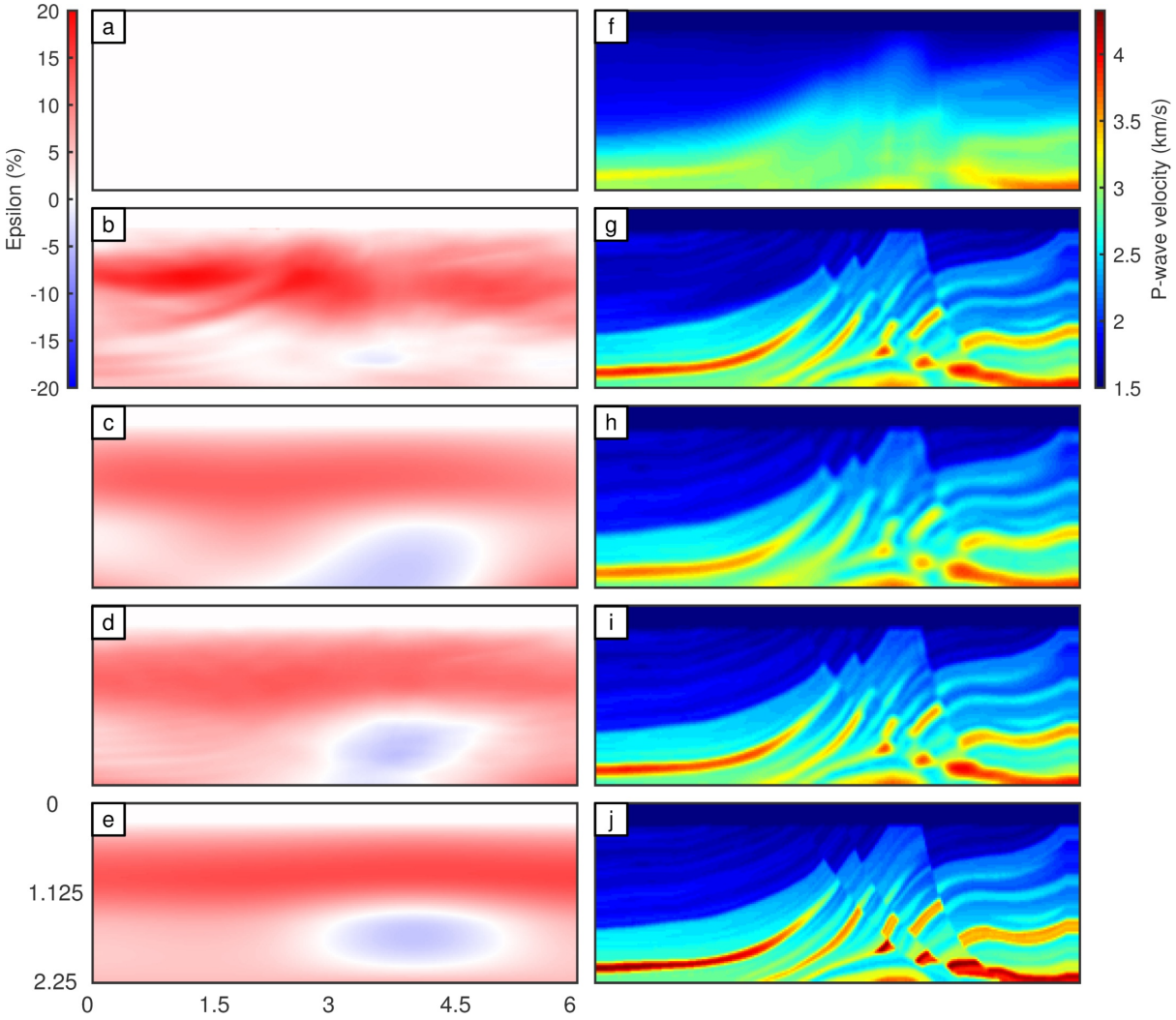


***Figure 2*** *Results from several multi-parameter inversions of surface seismic data from an anisotropic Marmousi model. (a) Start epsilon model; (b) local FWI epsilon model; (c) global epsilon model; (d) global epsilon model after additional local FWI update; (e) true epsilon model; (f) start P-wave velocity model; (g) local FWI P-wave velocity model; (h) global P-wave velocity model; (i) global P-wave velocity model after additional local FWI update; (j) true P-wave velocity model. Axes are in km.*

In these tests, 21 sources and 191 receivers were used, distributed evenly across the top of the model, using a Ricker source wavelet with a peak frequency of 6 Hz. The model, 2.25 km deep and 6 km wide, was sampled spatially every 25 m on a regular grid, while the data were sampled temporally every 2 ms. The anisotropic time-domain FWI algorithm used was that of Umpleby and Warner (2015), using a

multi-scale approach from 2 to 11 Hz over 100 iterations. The global inversion used a reduced bandwidth from 2 to 6 Hz. No prior assumptions were made for epsilon (Figure 2a), whilst a start model with no high-wavenumber information was provided for P-wave velocity (Figure 2f).

**Results**

The results of three different inversions can be seen in Figure 2, together with the true and start models for each parameter involved. As can be seen in Figure 2b, conventional simultaneous local FWI alone does a somewhat satisfactory job of delineating the high epsilon layer, capturing its shape and intensity well, but allowing noticeable high-wavenumber cross-talk to leak from the velocity model. This can also be seen clearly on individual traces (Figure 3a). Local FWI appears to struggle deeper in the model, where data coverage is less good, constructing only a vague outline of the low epsilon anomaly. The respective P-wave velocity model appears satisfactory (Figure 2g) but it also bears subtle scars from the cross-talk, which is most noticeable on the traces (Figure 3b).

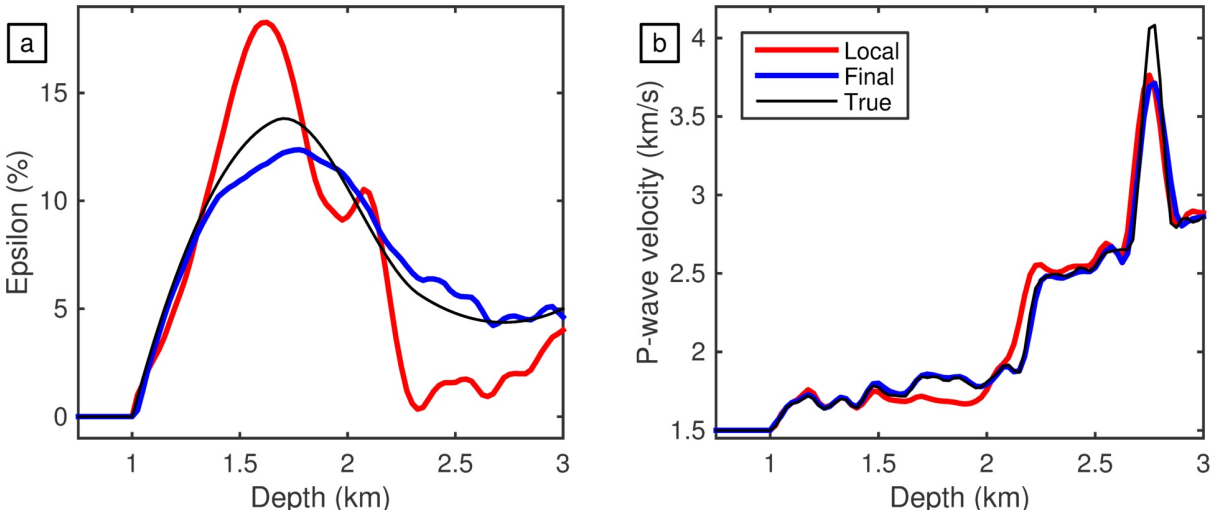


***Figure 3*** *Model trace comparisons at position 1.5 km for: (a) epsilon, and (b) P-wave velocity. Thin black lines indicate the true models, thick red lines indicate the local FWI results, and thick blue lines indicate models produced by the global approach followed by a local FWI update. Note how, in the region of the anisotropy model overestimated by local FWI, the corresponding velocity is underestimated, suggesting a trade-off between the two parameters.*

Figure 2c shows the resultant epsilon model from the global approach. While this does not capture the intensity of the high epsilon layer quite as well as local FWI, it does capture the form and structure of the model well throughout, even at depth. It is clear that this model is very likely to lie within the region of the global minimum of the inverse problem, and so should provide a desirable starting model for subsequent local FWI. The result of this can be seen in Figure 2d, where local FWI has served to tighten and improve the intensities of the features of the epsilon model, resulting in a solution that is close to the true model (Figure 2e). By using the velocity model produced by the global scheme (Figure 2h) for subsequent local FWI, an improved result is also obtained for the P-wave velocity (Figure 2i).

Figure 4 depicts three normalised misfit diagnostics produced during the progression of the global inversion. It can be seen that the best-fitting epsilon model rapidly converges to a minimum, stabilising after only about 10 generations, whilst the corresponding P-wave velocity-model misfit improves at a more gradual yet continuous rate. Based on the rapid convergence of the global inversion, it is clear that only about half as many generations as were used here would suffice. The breaks in the data misfit in Figure 4 represent jumps in the upper bound of the frequencies that are used to drive the inversion.

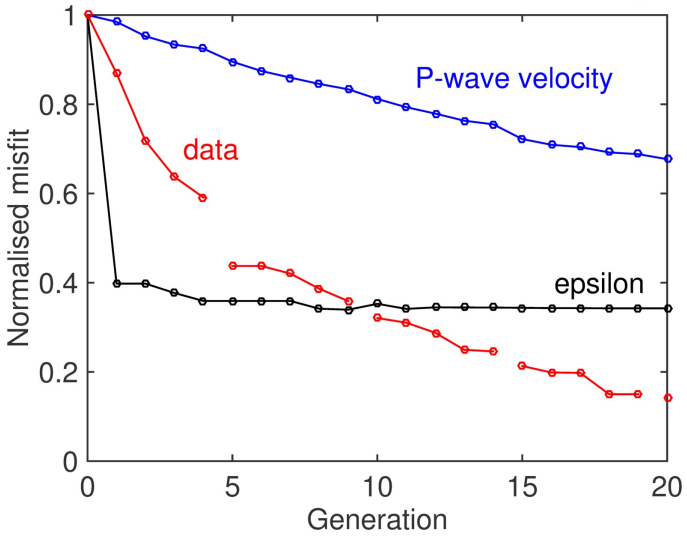


***Figure 4*** *Normalised misfit over successive generations for the global inversion described for the Marmousi example. The black line represents model misfit for the anisotropy model, the blue line model misfit for the velocity model, and the red line data misfit. The breaks in the data misfit indicate jumps in the frequency band used for the inversion.*

## Discussion and Conclusion

We have presented a hybrid inversion scheme, for surface seismic data, that combines global inversion for anisotropy with local inversion for P-wave velocity. This technique extracts the long-wavelength behaviour of the anisotropy during global inversion, and then subsequently improves the velocity model at high resolution using conventional local FWI. Our methodology has been demonstrated with the use of the synthetic Marmousi model. The approach appears to suppress cross-talk between the two inverted parameters, thus producing cleaner, more-accurate results for both models. Because the global inversion runs at only low frequency, and uses only three local iterations per global iteration, use of this hybrid inversion scheme dos not add significantly to the total cost of undertaking anisotropic FWI.

It is also possible to invert for anisotropy tilt angle using this approach, and specifically to invert for the degree to which the anisotropy is aligned with the vertical, with the stratigraphy, or with a local stress model. This approach to inverting for tilt angle requires only sparse parameterisation. It is extremely difficult to recover tilt angles using purely local inversion, but it is inexpensive and straightforward to achieve this with the global optimisation scheme outlined here.

## Acknowledgements

The authors are grateful to the sponsors of the Fullwave Game Changer consortium for supporting this work.

## References

Bourgeois, A., Bourget, M., Lailly, P., Poulet, M., Ricarte, P. and Versteeg, R. [1990] Marmousi, model and data. In: *Proceedings of the 1990 EAEG Workshop - Practical Aspects of Seismic Data Inversion*, Copenhagen, 5-16.

da Silva, N.V., Ratcliffe, A., Conroy, G., Vinje, V. and Body, G. [2014] A new parameterization for anisotropy update in full waveform inversion. *2014 SEG Annual Meeting*, Expanded Abstracts, Denver, 1050-1055.

Ji, Y. and Singh, S.C. [2005] Anisotropy from full waveform inversion of multicomponent seismic data using a hybrid optimization method. *Geophysical Prospecting*, **53**(3), 435-445.

Thomsen, L. [1986] Weak elastic anisotropy. *Geophysics*, **51**(10), 1954-1966.

Sun, J., Feng, B. and Xu, W. [2004] Particle swarm optimisation with particles having quantum behaviour. In: *Proceedings of the 2004 IEEE Congress on Evolutionary Computation*, Portland, 325-331.

Umpleby, A. and Warner, M.R. [2015] Robust recovery of anisotropy during full-waveform inversion. *77th EAGE Conference & Exhibition*, Extended Abstracts, Madrid.